

Application of carbon nanofiber films for gas sensors NO₂

© V. Golovakhin,¹ A.A. Shishin,¹ A.D. Lozben,¹ A.R. Smagulova,¹ T.S. Gudyma,¹
E.A. Maksimovskiy,² P.B. Kurmashov,¹ A.G. Bannov¹

¹ Novosibirsk State Technical University,
630073 Novosibirsk, Russia

² Nikolaev Institute of Inorganic Chemistry, Siberian Branch, Russian Academy of Sciences,
630090 Novosibirsk, Russia
e-mail: golovaxin-valera@mail.ru

Received October 3, 2024

Revised October 3, 2024

Accepted October 3, 2024

The selection of the optimal parameters for application and study of the carbon nanofiber films for gas sensors NO₂ was considered. The impact of time of ultrasonic dispersion of the suspension, mass of carbon nanofibers, volume of solvent was studied to apply the nanofiber-ethanol suspension on the sensor substrate using drop casting technique. Regression equations were produced, which determine the area of rational parameters, where it is necessary to apply the coating to obtain higher relative response of the sensor.

Keywords: carbon nanofibers, gas sensors, experiment design matrix, carbon material films.

DOI: 10.61011/TP.2025.03.60854.300-24

Introduction

Development of the global industry and increasing number of vehicles cause more emissions of hazardous gases to atmosphere [1,2]. The impact of these gases at the human body is negative even at low concentrations. Therefore it becomes increasingly necessary to develop effective methods of quick and selective detection of toxic and fire hazardous gases [3,4]. Despite the presence of many physical and chemical methods to detect substances in a gas phase, the design of the devices for monitoring of the environment condition and air in industrial areas remains a relevant task. One of such areas includes development of gas sensors [5–12]. Gas sensors — is one of the areas for potential use of carbon nanomaterials (CNM) [9–11], together with the applications as electrodes of supercapacitors [9,10], fillers for membranes [7,8] in composites with metals [13,14] and many more. If we consider sensors on their basis, two main types are most common in the scientific literature: chemiresistors and field effect transistor sensors (FET sensors). Moreover, there are also chemicapacitive sensors [15], surface acoustic wave sensors [16], optic fiber sensors [17] and quartz crystal microbalance sensors [18], but little attention is still paid to the issues of application of carbon nanomaterials for the sensors. Recently more and more attention is paid specifically to chemiresistors, as more functional, cheap and simple. Today the chemiresistors are made on the basis of semiconductors and differ with a comparatively small response (relative gas sensitivity) in respect to gases. Their another disadvantage is the condition of operation at material temperatures above 200 °C–250 °C [19], which is rather ineffective, especially in the area of integration into mobile/portable devices and analyzers, which require low

energy consumption (including for the objectives of exhaled air analysis [20]). Besides, there are certain problems related to the need for such high temperature, which increase explosion and fire risk of such devices. A novel approach is to design sensors based on CNM (carbon nanotubes, carbon nanofibers, graphene, reduced graphene oxide etc.). If the range of operation is considered (temperature of active material layer) for the sensors based on CNM, it is believed that they are stable in the range of 25 °C–250 °C [21], but most often such materials are used as room temperature sensors [22,23]. It is assumed that the gas sensors based on most CNM have much higher quick action compared to semiconductor ones [24] and the detection limit, which in certain cases may reach the levels of tens and hundreds ppb [25].

Main gases that the devices above may be oriented at are NH₃ [26–33], NO₂ [34,35], CH₄ [36,37], H₂ [38], H₂S [39–42], CO₂ [43] and others. The most promising area is the development of gas sensors to detect some key hazardous compounds: ammonia, hydrocarbons, nitrogen dioxide, volatile organic compounds. That is why the environmental monitoring using such sensors makes it possible to identify leaks and confine dangerous effects of such gas. One of such gases is NO₂. Increase of its concentration in the air of industrial enterprises may be lethal and cause certain diseases in the personnel. Besides, nitrogen dioxide is a corrosion-active gas, which may cause damage of the equipment elements and reduce the level of industrial safety. The objectives of nitrogen dioxide concentration monitoring in the ambient air (urban environment air) are also important. Therefore, the important task is to create a sensor, the relative response of which will be as high as possible in a combination with all other characteristics (low actuation time, low detection limit, high selectivity etc.).

The promising CNMs for the gas sensors NO₂ include carbon nanofibers (CNFs), which have a wide spectrum of applications due to their structure and properties [44–49]. Use of CNFs as an active materials in gas chemiresistors is a relevant task due to higher yield in their production and low cost compared to carbon nanotubes (CNTs), and also the ability to produce the material in the form of granules [15–17].

CNFs in the sensors may be applied on the substrates in the form of films by spin coating [18–20], drop casting [21–24] technique, and also when applied on dielectric substrates by CVD (chemical vapor deposition) and PECVD (plasma-enhanced chemical vapor deposition) methods [50–54]. Most studies in this area are focused on using new materials for gas sensors [24], while little attention is paid to optimization of parameters for application of the carbon material on a dielectric substrate. For the scaled production of sensors with CNF films as an active layer, it is necessary to analyze the parameters of material application on the sensor substrate and their gas sensitive properties. There are practically no papers dedicated to study of the contribution of the parameters for application of CNTs and CNFs [55].

This paper studied the process of film application by the drop casting technique. To assess the area of rational parameters of application, regression analysis was performed. Regression equations were produced, which indicate the area of parameters to be used for application. It is shown that not only the type of the carbon material may be changed when developing a sensor, but the method of its application onto the dielectric substrates as such, since this is quite a cheap and fast method to optimize the relative response of the sensors in respect to the nitrogen dioxide.

1. Materials and methods

1.1. CNFs

To prepare the active layer of the sensor, CNF samples produced by catalytic decomposition of methane (gas flow rate 550 l/h, process temperature — 550 °C) on a catalyst 90 % Ni/10 % Al₂O₃ in the pilot vibrofluidized bed reactor were taken. The process of synthesis was described in more detail in paper [56]. The feature of the process is production of CNFs in the form of granules, which are formed by vibration fluidization is used on a catalyst with high content of active component, providing for higher rate of carbon growth on Ni nanoparticles. These factors result in formation of not a powdered material, but granules that consist of tightly interwoven CNFs.

1.2. Method to produce CNF-based films

To develop the gas sensors, the CNF sample was not exposed to any special chemical treatment, therefore material contribution to the sensor properties is formed specifically by its initial physical and chemical properties

and the method of its application onto the substrates. The objectives of searching for the rational parameters of the CNF application onto the laminated fabric substrate (i.e. textolite) for the nitrogen dioxide sensor were solved using the planning of the experiment and the regression analysis [57]. This paper studied the effect of three factors at the relative response of the gas sensors in the range of concentrations of the analyzed gas 10–50 ppm. An experimental design matrix was made of 2³ type, and experiments were conducted under the plan of the complete factorial experiment [57,58]. It should be noted that each experiment for film production was reproduced three times to obtain a statistically significant value. All the estimates done to search for the optimal conditions were carried out under paper [58]. Since the sorting of all parameters of application causes significant number of experiments, the planning made it possible to reduce the number of experiments and to obtain the regression equations that relate the relative response of the sensors and parameters of its application.

In this paper the relative response of ($\Delta R/R_0, \%$) gas sensors vs NO₂ concentration was affected by such factors as (variation intervals are indicated as x_i^+, x_i^-):

- x_1 — time of ultrasonic dispersion of the suspension (τ , min), $x_1^+ = 30$, $x_1^- = 10$;
- x_2 — CNF weight (m , g), $x_2^+ = 0.08$, $x_2^- = 0.04$;
- x_3 — solvent volume (V , mL), $x_3^+ = 20$, $x_3^- = 10$.

Experimental design matrices are shown in the Annex.

The method of CNF application in the substrate was the following. To prepare the active layer of the sensor NO₂, first a CNF weight portion was taken with fraction below 80 μ m and constant mass, which was exposed to the ultrasonic dispersion in a bath UZV-3/200 (RELTEK, Russia) with the power of 85 W at frequency of 22 kHz for 10–30 min in ethanol (97 %).

Using the drop casting technique, the finished suspension was applied onto the surface of the preheated substrate at heating temperature of 80 °C. The gas sensor substrate was a base of laminated fabric with the copper contacts applied on the edges of the upper side. The substrates were mechanically polished by sand paper and cleaned with ethanol solution. To obtain the films of one geometry by suspension drop casting, a template 5 × 5 mm was used, which partially coats the copper contacts. The photographs of the gas sensor substrate are presented in fig. 1.

1.3. Measurement procedure

Relative response of the gas sensors was studied by a unit of dynamic type. For a detailed description, see [46]. This unit comprised five gas channels. To measure the value of gas sensors response, synthetic air (79 % N₂, 21 % O₂) was used as a carrier gas, and the analyzed gas was — NO₂. The main parameter is the relative response of the sensor (%):

$$\frac{\Delta R}{R_0} = \frac{R - R_0}{R_0} \cdot 100 \%,$$

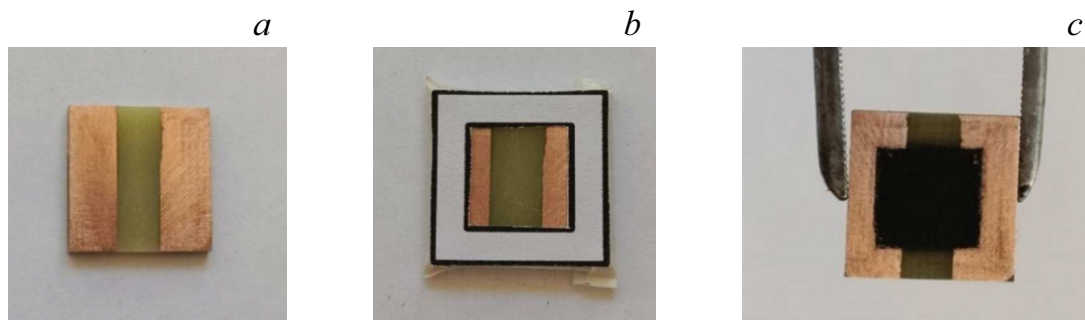


Figure 1. Photographs of the gas sensor substrate: *a* — polished substrate; *b* — template that partially coats the copper contacts; *c* — CNF film produced by drop casting technique.

where R — sensor resistance when exposed to analyzed gas, (Ω); R_0 — sensor resistance when exposed to carrier gas, (Ω). Sensor testing was carried out at temperature $25 \pm 2^\circ\text{C}$.

The studies were carried out in a cell by two-contact method (Keithley 2401 Source Meter). Data were collected by KickStart software.

Prior to the measurement, the empty closed cell was blown with carrier gas for 5 min with the gas flow rate of 200 mL/min. To desorb the gas molecules from the surface of the carbon material, the specimen was placed into the cell, and for 30 min the carrier gas was supplied with the flow rate of 100 mL/min and sensor heating temperature 70°C . After degassing the cell with the specimen was cooled for 30 min at the following gas flow rates: the first 25 min — with flow rate of 500 mL/min and for the remaining 5 min — with flow rate of 100 mL/min. Since the electrical resistance of the sensor in the air medium varied, the basic line $R(\tau)$ was measured for its subsequent subtraction from the experimental data when nitrogen dioxide is supplied. Further the basic line was measured when the carrier gas was supplied for 60 min with flow rate of 100 mL/min. After measurement of the basic line for 10 min, analyzed gas (NO_2 in air with certain concentration) was supplied to the cell, and then for 10 min — pure carrier gas for blowdown of the system and recovery of the sensor. Therefore, three cycles of the mix NO_2 /air were supplied, which were separated by carrier gas (air) supply cycles.

The studies of the sensor response to the action of NO_2 in the air medium were carried out at room temperature ($25 \pm 2^\circ\text{C}$) in the range of concentrations 10–50 ppm (relative air humidity $2 \pm 0.5\%$).

1.4. CNF properties

The CNF sample was studied using transmission electron microscopy (TEM) on electron microscope JEM-2010 (JEOL, Japan) at accelerating voltage of 200 kV and grid resolution of 0.14 nm. Texture characteristics of CNF were identified on adsorption unit Quantachrome NOVA 1000e using the method of low-temperature nitrogen adsorption

(77 K). Partial pressure of adsorbate gas (P/P_0) was in the range of 0.005–0.9995. To remove adsorption gases and moisture from the specimens prior to the analysis, CNF were exposed to vacuum at 130°C for 12 h.

The morphology of the CNF films on the substrate were assessed with scanning electron microscopy (SEM) S-3400N (Hitachi).

2. Results and discussion

2.1. CNF physical and chemical properties

TEM microphotographs of CNFs are shown in fig. 2.

The CNF sample is a material with a „fish bone“ structure with diameter of 15–100 nm. The length of the studied nanofibers reaches around several micrometers. The specific surface of the studied specimen by the method of low-temperature nitrogen adsorption was $119\text{ m}^2/\text{g}$ with preferential contribution of mesopores (specific surface of micropores — $3\text{ m}^2/\text{g}$). The mean size of the pores was 8.9 nm. The average diameter of nanofibers determined by analysis of microphotographs was $37.0 \pm 5.9\text{ nm}$.

SEM microphotographs of CNF films on the laminated fabric substrate are shown in fig. 3.

Following the SEM, the thickness of the CNF film layer varies in the range of 128–180 μm . Based on fig. 3, one may note that in the images (fig. 3, *b, d*) the films have a denser layer, and in the images (fig. 3, *a, c*) — uneven layer. The difference may be explained by the fact that at longer time of CNF suspension dispersion the size of the produced particles is much less and, therefore, the particles are packed more tightly when the suspension is applied onto the substrate.

2.2. Experiment planning and regression equations

Typical dependences of relative response of gas sensors vs NO_2 concentration qualitatively demonstrated the contribution of the application conditions to the change in the electrical resistance of the sensors when in contact with nitrogen dioxide at room temperature (fig. 4).

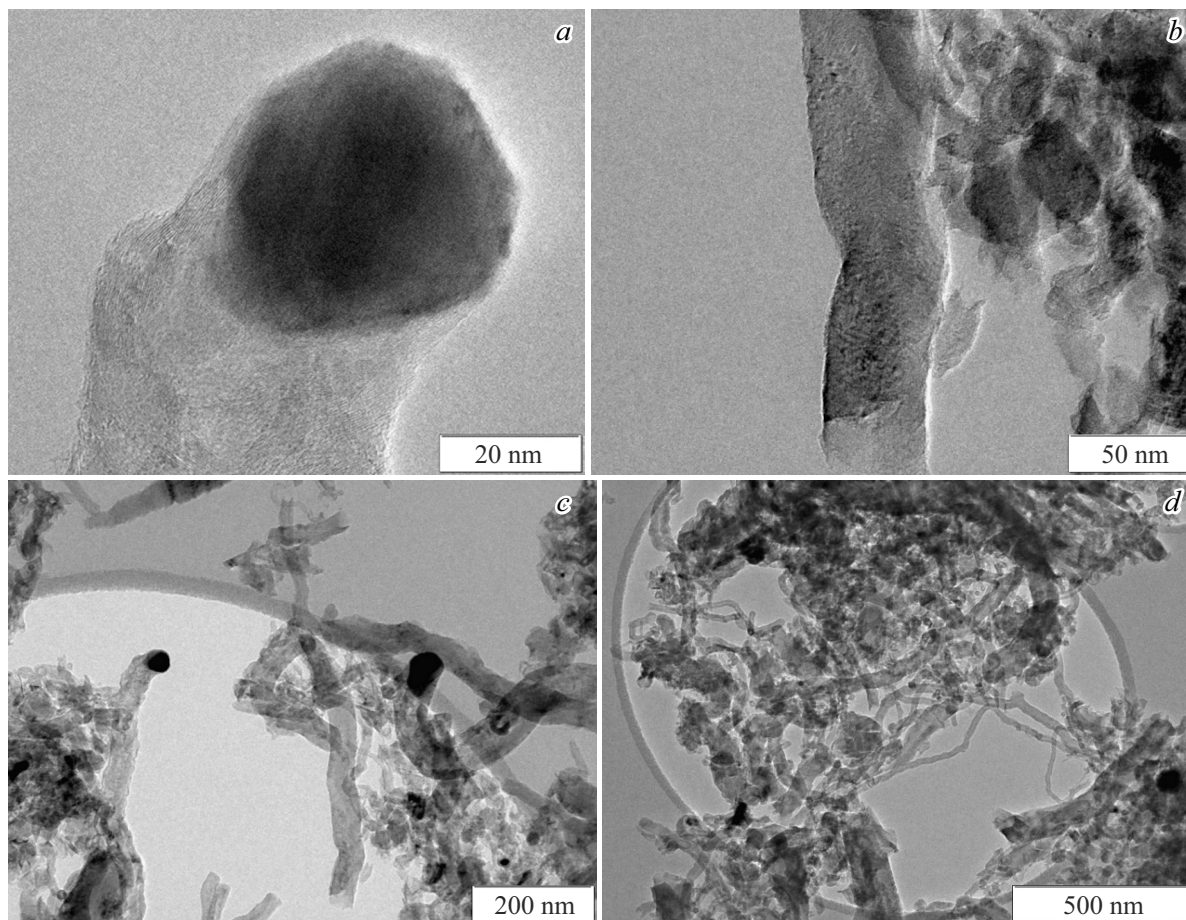
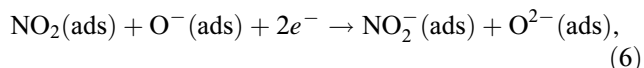
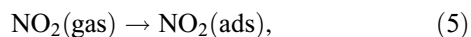
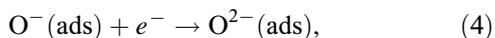
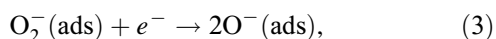
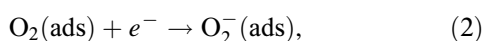
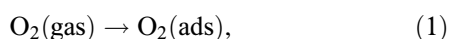


Figure 2. TEM microphotographs of CNF samples.

The mechanism of adsorption of NO_2 with carbon material may be presented as follows [59]:



Equation (1) describes interaction of oxygen from supplied air with carbon. Equations (2)–(4) show the transfer of electrons from the conduction band to oxygen to form negatively charged oxygen ions. Equation (5) describes interaction of nitrogen dioxide with carbon. Then equation (6) shows how the adsorbed NO_2 interacts with the negatively charged oxygen ion and electrons from the conductive layer. Equation (7) shows the interaction of detected gas with the previously formed oxygen ions to form NO_3^- .

In process of the calculations, the regression equation was made (with account of all interactions of factors), the dispersion was studied for its homogeneity by Cochran criterion, and the produced model was tested for adequacy. Experimental design matrices and experiment results are given in Annex.

Electrical resistance of gas sensors, which were studied, reduced when in contact with nitrogen oxide. Such behavior is typical for carbon materials when in contact with the electron-acceptor gas [60]. When the nitrogen dioxide is adsorbed on the carbon surface, electron concentration reduces in the surface layer of the material, and the concentration of charge carriers in CNF (holes) increases, causing electrical resistance to drop [61,62]. Relative response of gas sensors ΔR varied from 2% at 10 ppm to 40% at 50 ppm. Sensitivity of such sensors is higher compared to the sensors based on various materials, including polypyrrole [63], ozone-functionalized graphene [64], reduced oxyfluorinated graphite [65], fluorinated graphene films [66] etc.

Let us further consider the experiment planning and its results. For each factor there is a center of plan x_i^0 (middle of the range between the lower and upper intervals of

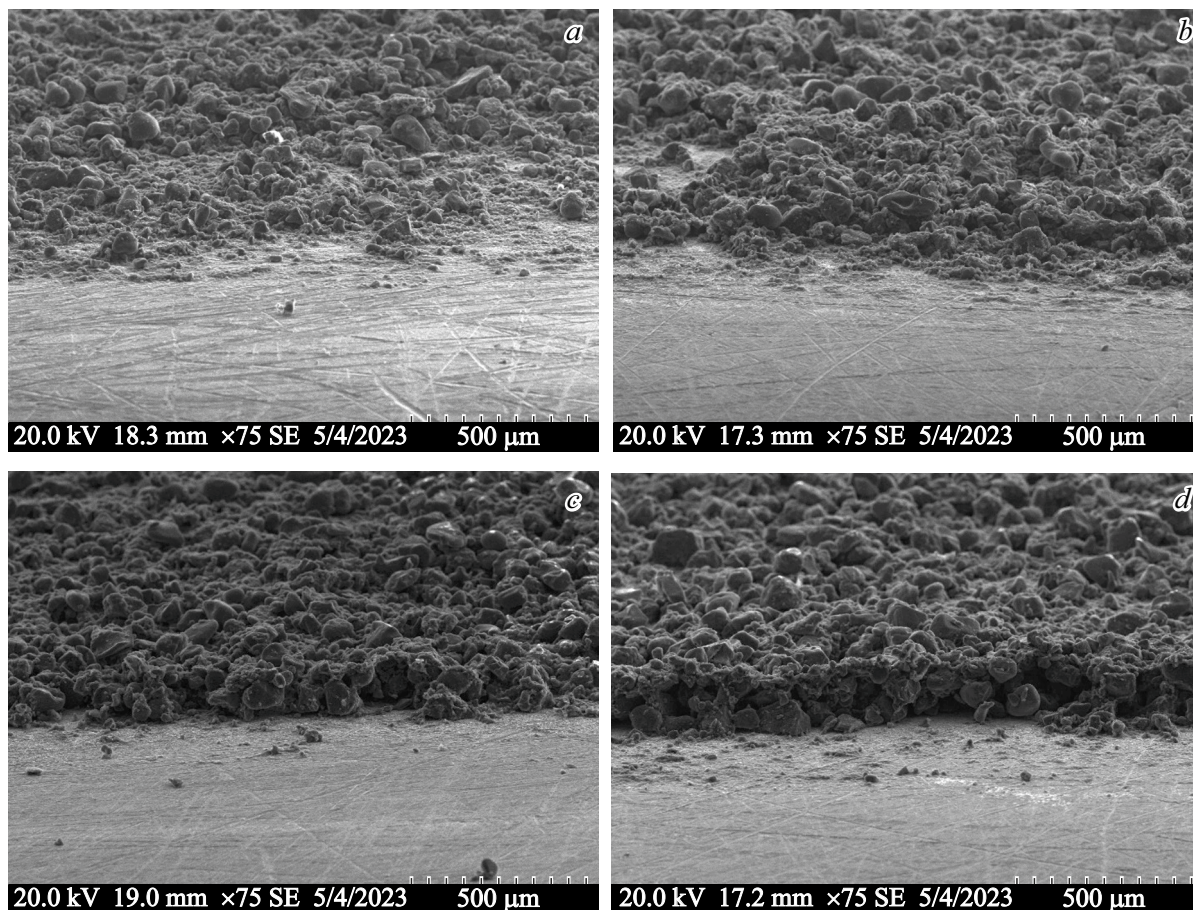


Figure 3. SEM images of CNF films (parameters: CNF weight, time of suspension dispersion, solvent volume): *a* — 40 mg, 10 min, 10 mL; *b* — 40 mg, 30 min, 10 mL; *c* — 80 mg, 10 min, 20 mL; *d* — 80 mg, 30 min, 10 mL.

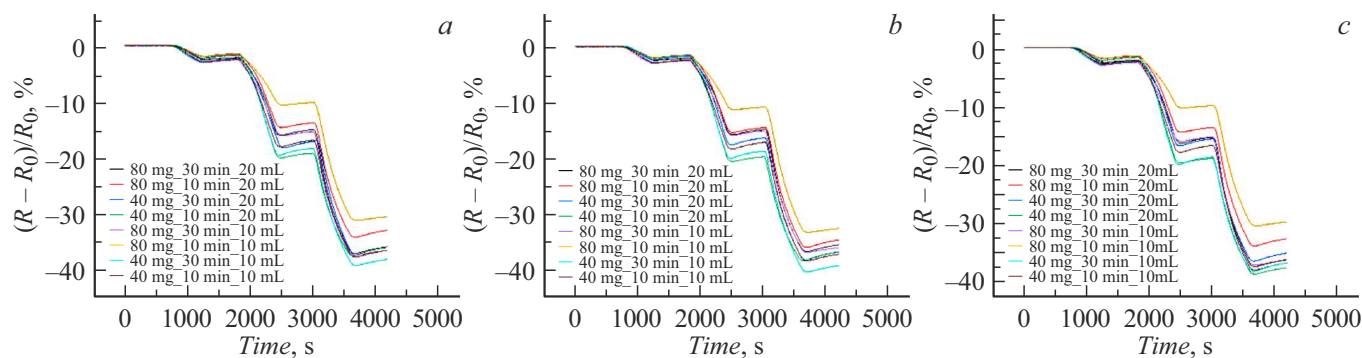


Figure 4. Dependences of relative response of CNF films on 10, 25, 50 ppm NO₂ at (25 ± 1) °C (duration of feed cycle of mix NO₂-air — 10 min; cycles are separated from each other by pure air supply for 10 min): *a* — CNF film response in the first series of experiments; *b* — CNF film response in the second series of experiments; *c* — CNF film response in the third series of experiments.

variation x_i^+ and x_i^-) and variation interval λ_i :

$$x_i^0 = \frac{x_i^+ + x_i^-}{2}, \tag{8}$$

where x_i^+ — upper level of the factor; x_i^- — lower level of the factor.

$$\lambda_i = \frac{x_i^+ - x_i^-}{2}. \tag{9}$$

The calculation results for other factors are given in table 1.

Let us consider the impact of variation of the optimization parameters separately for each concentration (10, 25, 50 ppm) of the analyzed gas supplied to the cell NO₂.

Below you can see the example of calculation for the data collected at relative response at 10 ppm. For the given measurement results (see Annex, table 2) of the

Table 1. Experimental design matrix for result processing

No. of experiment	Factors			Response, %								
	x_1	x_2	x_3	1st series of experiments			2nd series of experiments			3rd series of experiments		
	$t, \text{ min}$	$m, \text{ g}$	$V, \text{ mL}$	10 ppm	25 ppm	50 ppm	10 ppm	25 ppm	50 ppm	10 ppm	25 ppm	50 ppm
1	30	0.08	20	-2.568	-16.065	-37.324	-3.483	-13.975	-36.684	-2.595	-15.389	-38.087
2	10	0.08	20	-1.949	-15.421	-34.447	-2.025	-13.366	-35.983	-1.88	-14.491	-33.916
3	30	0.04	20	-2.356	-18.191	-37.335	-3.388	-15.565	-38.223	-2.272	-16.828	-36.545
4	10	0.04	20	-2.226	-19.666	-37.727	-2.126	-18.757	-35.971	-2.249	-19.972	-38.321
5	30	0.08	10	-3.112	-16.241	-37.621	-4.016	-14.873	-36.849	-3.04	-15.879	-37.221
6	10	0.08	10	-1.905	-10.654	-31.394	-2.013	-9.293	-33.285	-1.853	-12.343	-30.474
7	30	0.04	10	-2.948	-19.128	-39.485	-3.006	-17.569	-40.362	-2.921	-20.437	-38.846
8	10	0.04	10	-2.933	-18.167	-37.962	-2.938	-17.337	-38.396	-2.861	-17.926	-36.432

Table 2. Experimental design matrix for treatment of the results at 10 ppm

No. of experiment	Factors			Interactions				Response, %			
	x_1	x_2	x_3	x_1x_2	x_1x_3	x_2x_3	$x_1x_2x_3$	10 ppm	10 ppm	10 ppm	\bar{y}
	$t, \text{ min}$	$m, \text{ g}$	$V, \text{ mL}$					10 ppm	10 ppm	10 ppm	\bar{y}
1	(+) 30	(+) 0.08	(+) 20	+	+	+	+	-2.568	-3.483	-2.595	-2.882
2	(-) 10	(+) 0.08	(+) 20	-	-	+	-	-1.949	-2.025	-1.88	-1.951
3	(+) 30	(-) 0.04	(+) 20	-	+	-	-	-2.356	-3.388	-2.272	-2.672
4	(-) 10	(-) 0.04	(+) 20	+	-	-	+	-2.226	-2.126	-2.249	-2.200
5	(+) 30	(+) 0.08	(-) 10	+	-	-	-	-3.112	-4.016	-3.04	-3.389
6	(-) 10	(+) 0.08	(-) 10	-	+	-	+	-1.905	-2.013	-1.853	-1.924
7	(+) 30	(-) 0.04	(-) 10	-	-	+	+	-2.948	-3.006	-2.921	-2.958
8	(-) 10	(-) 0.04	(-) 10	+	+	+	-	-2.933	-2.938	-2.861	-2.911

concentration response 10 ppm we found the average values of relative response:

$$\bar{y} = \frac{1}{n} \cdot \sum_{i,j=1}^n y_{ji}, \tag{10}$$

where n — number of parallel experiments; y_{ji} — result of a separate experiment (i th experiment in j th experiment).

Results of the calculation for the other concentrations are given in table 3 and 4 of the Annex. The linear regression equation model with account of paired interactions of different factors looks as follows:

$$\hat{y} = b_0 + b_1x_1 + b_2x_2 + b_3x_3 + b_{12}x_1x_2 + b_{13}x_1x_3 + b_{23}x_2x_3 + b_{123}x_1x_2x_3. \tag{11}$$

Coefficients of this equation were found by the least-square method:

$$b_0 = \frac{1}{N} \cdot \sum_{j=1}^N \bar{y}_j, \tag{12}$$

$$b_i = \frac{1}{N} \cdot \sum_{j=1}^N x_{ji} \bar{y}_j, \tag{13}$$

$$b_{q,p} = \frac{1}{N} \cdot \sum_{j=1}^N x_{jq} x_{jp} \bar{y}_j, \tag{14}$$

where N — number of experiments; $X_{j(i,q,p)}$ — vector-column (j — number of experiments and i, q, p — number of experiment); \bar{y}_j — average values of response in j th experiment.

The results of calculation for the other coefficients of the regression equation are given in table 2.

Table 3. Experimental design matrix of treatment of the results at 25 ppm

No. of experiment	Factors			Interactions				Response, %			
	x_1	x_2	x_3	x_1x_2	x_1x_3	x_2x_3	$x_1x_2x_3$	25 ppm	25 ppm	25 ppm	\bar{y}
	$t, \text{ min}$	$m, \text{ g}$	$V, \text{ mL}$								
1	(+) 30	(+) 0.08	(+) 20	+	+	+	+	-16.065	-13.975	-15.389	-15.143
2	(-) 10	(+) 0.08	(+) 20	-	-	+	-	-15.421	-13.366	-14.491	-14.426
3	(+) 30	(-) 0.04	(+) 20	-	+	-	-	-18.191	-15.565	-16.828	-16.861
4	(-) 10	(-) 0.04	(+) 20	+	-	-	+	-19.666	-18.757	-19.972	-19.465
5	(+) 30	(+) 0.08	(-) 10	+	-	-	-	-16.241	-14.873	-15.879	-15.664
6	(-) 10	(+) 0.08	(-) 10	-	+	-	+	-10.654	-9.293	-12.343	-10.763
7	(+) 30	(-) 0.04	(-) 10	-	-	+	+	-19.128	-17.569	-20.437	-19.045
8	(-) 10	(-) 0.04	(-) 10	+	+	+	-	-18.167	-17.337	-17.926	-17.810

Table 4. Experimental design matrix of treatment of the results at 50 ppm

No of experiment	Factors			Interactions				Response, %			
	x_1	x_2	x_3	x_1x_2	x_1x_3	x_2x_3	$x_1x_2x_3$	50 ppm	50 ppm	50 ppm	\bar{y}
	$t, \text{ min}$	$m, \text{ g}$	$V, \text{ mL}$								
1	(+) 30	(+) 0.08	(+) 20	+	+	+	+	-37.324	-36.684	-38.087	-37.365
2	(-) 10	(+) 0.08	(+) 20	-	-	+	-	-34.447	-35.983	-33.916	-34.782
3	(+) 30	(-) 0.04	(+) 20	-	+	-	-	-37.335	-38.223	-36.545	-37.368
4	(-) 10	(-) 0.04	(+) 20	+	-	-	+	-37.727	-35.971	-38.321	-37.340
5	(+) 30	(+) 0.08	(-) 10	+	-	-	-	-37.621	-36.849	-37.221	-37.230
6	(-) 10	(+) 0.08	(-) 10	-	+	-	+	-31.394	-33.285	-30.474	-31.718
7	(+) 30	(-) 0.04	(-) 10	-	-	+	+	-39.485	-40.362	-38.846	-39.564
8	(-) 10	(-) 0.04	(-) 10	+	+	+	-	-37.962	-38.396	-36.432	-37.597

Average values of relative response are given in table 3.

Results of the statistical calculation are presented in table 4.

Comparison of experimental and tabular values of the Cochran criterion for all three concentrations NO_2 confirms the hypothesis on the dispersion homogeneity, since the experimental values did not exceed the tabular ones. Comparison of the Fischer's criterion values F with their tabular values at the significance level $\alpha = 0.05$ showed that the estimated value is below the tabular one, and all three regression equations below are adequate. For all three regression equations the negligible coefficients were excluded, if their values b were less than the product of the Student's coefficient and mean square deviation $t \cdot S_{coef}$. Therefore, three regression equations were obtained, which connect the relative response $\Delta R/R_0$ and parameters of material application (for concentration of 10 ppm). Since

coefficients $b_2, b_{1,3}, b_{2,3}, b_{1,2,3} < 0.151$ (the product of the Student's coefficient and mean square deviation of coefficients), they were accepted as negligible and were not included into the regression equations. For concentration of 10 ppm we have the following:

$$\Delta R/R_0 = -2.611 - 0.364\tau + 0.185V - 0.235\tau m.$$

If we analyze the produced equation at concentration of 10 ppm NO_2 , we can note that at reduction of time of ultrasonic dispersion of suspension below 20 min and interaction of time of ultrasonic dispersion with CNF weight, the response of gas sensors will increase (since coefficients at τ and $\tau \cdot m$ for pair interaction — are negative). Increased volume of the solvent above 15 mL will cause increase in the response, and its drop — decrease (since the coefficient at x_3 is positive). The area of rational parameters will be within the following limits: dispersion time — 10 – 20 min;

solvent volume — 15–20 mL (CNF weight factor is not significant compared to other parameters).

For concentration of 25 ppm the equation will look like

$$\frac{\Delta R}{R_0} = -16.147 - 0.531\tau + 2.148m - 0.873\tau m + 1.003\tau V.$$

Similarly coefficients b_2 , $b_{2,3}$, $b_{1,2,3}$, smaller than 0.469, were excluded from the equation as negligible.

If we analyze the produced equation at concentration of 25 ppm NO₂, we can note that at increase of time parameters of ultrasonic dispersion of suspension and interaction of time of ultrasonic dispersion with CNF weight, the response of gas sensors will increase (since coefficients at τ and $\tau \cdot m$ — are negative). Increase of CNF weight above 60 mg and time of interaction of ultrasonic dispersion with the solvent volume will cause response increase. The area of the rational parameters will stay within the following limits: dispersion time — 10–20 min; CNF weight — 60–80 mg (solvent volume as a separate factor has no significant impact).

For concentration of 50 ppm the equation will look like

$$\frac{\Delta R}{R_0} = -36.620 - 1.261\tau + 1.347m - 0.763\tau m + 0.609\tau V - 0.707mV.$$

Similarly coefficients b_3 , $b_{1,2,3}$, smaller than 0.424, were excluded from the equation as negligible.

Note that with reduction of time of ultrasonic dispersion of the suspension (below 10 min), time of interaction of ultrasonic dispersion with CNF weight and CNF weight with the solvent volume, the response of gas sensors in respect to nitrogen dioxide will increase (since coefficients at τ , $\tau \cdot m$ and x_2x_3 are negative). Increase of CNF weight above 80 mg and factors of interaction of ultrasonic dispersion and time factors will cause increase in response, and their increase - to decrease (since the coefficients at m and $\tau \cdot V$ — are negative). The area of the rational parameters will stay within the following limits: dispersion time — 10–20 min; CNF weight — 60–80 mg (solvent volume as a separate factor has no significant impact).

Therefore, the common parameter to increase the relative response of dispersion is the duration of ultrasonic dispersion that should amount to 10–20 min. Shorter dispersion times act, evidently, softly to CNFs. The higher CNF weight causes viscous suspension and formation of films with higher thickness, i.e. long dispersion causes formation of thin films, which is not desirable for increase of the relative response. CNF weight increase and solvent volume decrease factors cause higher concentration of the suspension, which rightfully results in the formation of films with thickness ($\sim 150 \pm 25 \mu\text{m}$, fig. 3, *d*) compared to thinner films (fig. 3, *a-c*; for example, for fig. 3, *a, b* the coating thickness will not exceed 75–125 μm). Despite

higher electrical resistance of such CNF layers, relative response of such films will be higher compared to the layers of small thickness since the coating is porous, and gas penetrates in it, and therefore large surface is involved for adsorption.

Table 5 presents the comparison of relative response of the sensors with the published data, showing the efficiency of the sensors with the very simple method of CNF coating preparation, without modification of the material surface.

To conclude, we should say that such simple and cheap tool to manage the relative response of the sensors as the method of their application, may be used for some optimization of their characteristics. This paper produced and analyzed multiple specimens (24 sensors), and most measurements made it possible to make statistically adequate regression equations to describe the parameters of CNF application onto the substrates from laminated fabric by drop casting technique. Nitrogen dioxide response of the material may be increased, if you take into account the fact that this does not change the type of the sensitive material of the sensor, no chemical treatment is used, or other methods to improve the sensor parameters.

Conclusion

To prepare the gas sensors, the following parameters were selected: CNF weight (40 mg, 80 mg), solvent volume (10 mL, 20 mL), ultrasonic dispersion time (10 min, 30 min), which were used to make the complete factorial experiment design matrix 2³. It was found that impact of CNF application parameters on the substrates is not the same for various concentrations of NO₂, which must be identified. Experimental design results demonstrated that for concentration of NO₂ 10 ppm at reduction of suspension ultrasonic dispersion time parameters (10–20 min) and increase of solvent volume (15–20 mL), the response of the gas sensors will increase. For concentration of NO₂ 25–50 ppm at reduced time of ultrasonic dispersion of suspension (10–20 min) and increase of CNF weight in the suspension (60–80 mg), the response of the gas sensors will increase. It was shown that the parameters of carbon material application onto the substrate made it possible to manage the relative response of the gas sensor. Such approach requires no substitution of the active material of the sensor and differs by relative simplicity, requires no treatment of carbon material or any other actions.

Funding

The work was done under the state assignment of the Ministry of Science and Higher Education of the Russian Federation (FSUN-2023-0008).

Conflict of interest

The authors declare that they have no conflict of interest.

References

- [1] R.M. Usmanova, N.A. Sattarova, N.N. Boyko. IOP Conf. Ser. Mater. Sci. Eng., **1079**, 062040 (2021). DOI: 10.1088/1757-899X/1079/6/062040
- [2] I.D. Williams, M. Blyth. Sci. Total Environ., **858**, 159987 (2023). DOI: 10.1016/j.scitotenv.2022.159987
- [3] E. Llobet. Sensors and Actuators B: Chem., **179**, 32 (2013). DOI: 10.1016/j.snb.2012.11.014
- [4] R.B. Onyancha, K.E. Ukhurebor, U.O. Aigbe, O.A. Osibote, H.S. Kusuma, H. Darmokoesoemo, V.A. Balogun. Sensing and Bio-Sensing Research, **34**, 100463 (2021). DOI: 10.1016/j.sbsr.2021.100463
- [5] S. Freddi, M. Vergari, S. Pagliara, L. Sangalettiet. Sensors., **23** (2), 882 (2023). DOI: 10.3390/s23020882
- [6] M.A. Hejazi, O. Eksik, Ç. Taşdelen-Yücedağ, C. Ünlü, L. Trabzon. Emergent Mater., **6**, 45 (2023). DOI: 10.1007/s42247-023-00454-7
- [7] S. Shahzad, H. Wang, W. Li, Y. Sun, D. Xie, T. Ren. Chemosensors, **10** (3), 119 (2022). DOI: 10.3390/chemosensors10030119
- [8] L. Fu, A.M. Yu. Rev. Adv. Mater. Sci., **36**, 40 (2014).
- [9] B. De, S. Banerjee, T. Pal, K. D. Verma, A. Tyaga, P.K. Manna, K.K. Kar. Spr. Ser. Mat. Sc., **302**, 353 (2020). DOI: 10.1007/978-3-030-52359-6_14
- [10] D.K. Maurya, S. Angaiah. *Electrospun Nanofibers based Electrodes and Electrolytes for Supercapacitors*. In: A. Vaseashta, N. Bölgen (eds). *Electrospun Nanofibers* (Springer, Cham., 2022), DOI: 10.1007/978-3-030-99958-2_13
- [11] Y. Zhao, H. Bin, Y. Ji, Y. Yu, X. Gao, Zh. Zhang, H.-F. Fei. ACS Appl. Mater. Interfaces, **15** (4), 5644 (2023). DOI: 10.1021/acsami.2c19696
- [12] Y. Wang, J. Cui, Q. Qu, W. Ma, F. Li, W. Du, K. Liu, Q. Zhang, S. He, Ch. Huang. Microporous Mesoporous Mater. Elsevier Inc., **329**, 111545 (2022). DOI: 10.1016/j.micromeso.2021.111545
- [13] C. Vincent, J.M. Heintz, J.F. Silvain, N. Chandra. Open J. Compos. Mater., **1**, 1 (2011). DOI: 10.4236/ojcm.2011.11001
- [14] I. Sharafeldin, S. Garcia-Rios, N. Ahmed, M. Alvarado, X. Vilanova, N.K. Allam. J. Environ. Chem. Eng. Elsevier Ltd., **9** (1), 104534 (2021). DOI: 10.1016/j.jece.2020.104534
- [15] S. Kim, K.-H. Lee, J.Y. Lee, K.K. Kim, Y.-H. Choa, J.-H. Lim. Electron. Mater. Lett., **15**, 12 (2019). DOI: 10.1007/s13391-019-00177-0
- [16] Q.B. Tang, Y.J. Guo, Y.L. Tang, G.D. Long, J.L. Wang, D.J. Li, Xi.-T. Zu, J.Y. Ma, L. Wang, H. Torun, Y.Q. Fu. J. Mater. Sci., **54**, 11925 (2019). DOI: 10.1007/s10853-019-03764-6
- [17] C. Yu, Y. Wu, X. Liu, F. Fu, Y. Gong, Y. Rao, Y. Chen. Sensors Actuators, B Chem., **244**, 107 (2017). DOI: 10.1016/j.snb.2016.12.126
- [18] X. Li, C. Xiangdong, Y. Yao, Li Ning, C. Xinpeng. Sensors Actuators B: Chem., **196**, 183 (2014). DOI: 10.1016/j.snb.2014.01.088
- [19] M. Meyyappan. Small, **12** (16), 2118 (2016). DOI: 10.1002/sml.201502555
- [20] M. Kaloumenou, E. Skotadis, N. Lagopati, E. Efstathopoulos, D. Tsoukalas. Sensors., **22** (3), 1238 (2022). DOI: 10.3390/s22031238
- [21] L. Valentini, I. Armentano, J.M. Kenny, C. Cantalini, L. Lozzi, S. Santucci. Appl. Phys. Lett., **82**, 961 (2003). DOI: 10.1063/1.1545166
- [22] F. Usman, K.H. Ghazali, R. Muda, J.O. Dennis, K.H. Ibnaouf, O.A. Aldaghri, A. Alsadig, N.H. Johari, R. Jose. Chemosensors, **11** (2), 119 (2023). DOI: 10.3390/chemosensors11020119
- [23] S. Deng, V. Tjoa, H.M. Fan, H.R. Tan, D.C. Sayle, M. Olivo, S. Mhaisalkar, J. Wei, C.H. Sow. J. Am. Chem. Soc., **134** (10), 4905 (2012). DOI: 10.1021/ja211683m
- [24] R.G. Mendes, P.S. Wróbel, A. Bachmatiuk, J. Sun, Th. Gemming, Zh. Liu, M.H. Rüttmeli. Chemosensors, **6** (4), 60 (2018). DOI: 10.3390/chemosensors6040060
- [25] F. Zhang, Q. Lin, F. Han, Z. Wang, B. Tian, L. Zhao, T. Dong, Z. Jiang. Microsystems Nanoeng., **8**, Art. Num. 40 (2022). DOI: 10.1038/s41378-022-00369-z
- [26] L. Randeniya, P.J. Martin, A. Bendavid, J. McDonnell. Carbon, **49** (15), 5265 (2011). DOI: 10.1016/j.carbon.2011.07.044
- [27] X. Feng, S. Irle, H. Witek, K. Morokuma, R. Vidic, E. Borguet. J. Am. Chem. Soc., **127** (30), 10533 (2005). DOI: 10.1021/ja042998u
- [28] R. Mangu, S. Rajaputra, P. Clore, D. Qian, R. Andrews, V. Singh. Mater. Sci. Eng. B, **174** (1–3), 2 (2010). DOI: 10.1016/J.MSEB.2010.03.003
- [29] F. Rigoni, S. Tognolini, P. Borghetti, G. Drera, S. Pagliara, A. Goldonid, L. Sangalett. Analyst. **138** (24), 7392 (2013). DOI: 10.1039/c3an01209c
- [30] E. Bekyarova, M. Davis, T. Burch, M.E. Itkis, B. Zhao, S. Sunshine, R.C. Haddon. J. Phys. Chem. B, **108** (51), 19717 (2004). DOI: 10.1021/jp0471857
- [31] R.M. Sidek, F.A.M. Yusof, F.M. Yasin, R. Wagiran, F. Ahmadun. *Electrical response of multi-walled carbon nanotubes to ammonia and carbon dioxide*, 2010 IEEE Intern. Conf. Semiconductor Electron. (ICSE2010) (Malacca, Malaysia, 2010), p. 263–266. DOI: 10.1109/SMELEC.2010.5549502
- [32] J. Kombarakkaran, C.F.M. Clewett, T. Pietraß. Chem. Phys. Lett., **441** (4–6), 282 (2007). DOI: 10.1016/j.cplett.2007.05.015
- [33] J.-W. Han, B. Kim, B. Kim, J. Li, M. Meyyappan. RSC Adv., **4**, 549 (2014). DOI: 10.1039/c3ra46347h
- [34] A. Sharma, M. Tomar, V.J. Gupta. Mater. Chem., **22**, 23608 (2012). DOI: 10.1039/C2JM35172B
- [35] S. Peng, K. Cho, P. Qi, H. Dai. Chem. Phys. Lett., **387** (4–6), 271 (2004). DOI: 10.1016/j.cplett.2004.02.026
- [36] Z. Li, J. Li, X. Wu, S. Shuang, C. Dong, M.M.F. Choi. Sensors Actuators B Chem., **139** (2), 453 (2009). DOI: 10.1016/j.snb.2009.03.069
- [37] X. Li, J. Liu, C. Zhu. *Various characteristic of Carbon nanotubes film methane Gas sensor*, 1st IEEE Intern. Conf. on Nano/Micro Engineered and Molecular Systems (Zhuhai, China, 2006), p. 1453–1456. DOI: 10.1109/NEMS.2006.334805
- [38] P. Samarasekara. Chinese J. Phys., **47** (3), 361 (2009).
- [39] H. Dai, P. Xiao, Q. Lou. Phys. Status Solidi., **208** (7), 1714 (2011). DOI: 10.1002/pssa.201026562
- [40] H. Li, J. Zhang, G. Li, F. Tan, R. Liu, T. Zhang, H. Jin, Q. Li. Carbon, **66**, 369 (2014). DOI: 10.1016/j.carbon.2013.09.012

- [41] J. Mäklin, T. Mustonen, N. Halonen, G. Toth, K. Kordás, J. Vähäkangas, H. Moilanen, A. Kukovecz, Z. Kónya, H. Haspel, Z. Gingl, P. Heszler, R. Vajtai, P.M. Ajayan. *Phys. Status Solidi Basic Res.*, **245** (10), 2335 (2008). DOI: 10.1002/pssb.200879580
- [42] F. Mendoza, D. Hernández, V. Makarov, E. Febus, B. Weiner, G. Morell. *Sensors Actuators B: Chem.*, **190**, 227 (2014). DOI: 10.1016/j.snb.2013.08.050
- [43] K.G. Ong, C. Grimes. *Sensors*, **1** (6), 193 (2001). DOI: 10.3390/s10600193
- [44] V. Desmaris, M.A. Saleem, S. Shafiee. *IEEE Nanotechnol. Mag.*, **9** (3), 33 (2015). DOI: 10.1109/MNANO.2015.2409394
- [45] Z. Wang, S. Wu, J. Wang, A. Yu, G. Wei. *Nanomaterials*, **9** (7), 1045 (2019). DOI: 10.3390/nano9071045
- [46] A.G. Bannov, N.I. Lapekin, P.B. Kurmashov, A.V. Ukhina A. Manakhov. *Chemosensors*, **10** (12), 525 (2022). DOI: 10.3390/chemosensors10120525
- [47] P. Dariyal, S. Sharma, G.S. Chauhan, B.P. Singh, S.R. Dhakate. *Nanoscale Adv. Royal Society Chem.*, **3**, 6514 (2021). DOI: 10.1039/D1NA00707F
- [48] M. Clausi, M.G. Santonicola, S. Laurenzi. *Compos. Part A: Appl. Sci. Manuf.*, **88**, 86 (2016). DOI: 10.1016/j.compositesa.2016.05.026
- [49] R.K. Yonkoski, D.S. Soane. *J. Appl. Phys.*, **72**, 725 (1992). DOI: 10.1063/1.351859
- [50] T. Ohara, Y. Matsumoto, H. Ohashi. *Phys. Fluids A.*, **1**, 1949 (1989). DOI: 10.1063/1.857520
- [51] C.J. Venegas, S. Bollo, P. Sierra-Rosales. *Micromachines*, **14** (9), 1752 (2023). DOI: 10.3390/mi14091752
- [52] W. Boumya, N. Taoufik, M. Achak, N. Barka. *J. Pharm. Anal.*, **11** (2), 138 (2021). DOI: 10.1016/j.jpha.2020.11.003
- [53] O. Kanoun, C. Müller, A. Benchirouf, A. Sanli, T.N. Dinh, A. Al-Hamry, L. Bu, C. Gerlach, A. Bouhamed. *Sensors*, **14** (6), 10042 (2014). DOI: 10.3390/s140610042
- [54] A.G. Bannov, O. Jašek, J. Prášek, J. Buršík, L. Zajíčková. *J. Sensors*, **2018**, 7497619 (2018). DOI: 10.1155/2018/7497619
- [55] J.T.W. Yeow, Y. Wang. *J. Sensors*, **2009**, 493904 (2009). DOI: 10.1155/2009/493904
- [56] P.B. Kurmashov, V.V. Maksimenko, A.G. Bannov, G.G. Kuvshinov. *Gorizontalny pilotny reaktor s vibroozhizhenym sloem dlya protsessa sinteza nanovoloknistogo ugleroda. Khimicheskaya tekhnologiya* (BGTU Minsk, 2013), s. 635–640 (in Russian).
- [57] N.R. Draper, H. Smith. *Applied Regression Analysis* (Wiley, 1998)
- [58] Yu.P. Adler, E.V. Markova, Yu.V. Granovsky. *Planirovanie eksperimenta pri poiske optimalnykh usloviy* (Nauka, M., 1976), s. 280 (in Russian).
- [59] S. Drewniak, Ł. Drewniak, T. Pustelny. *Sensors*, **22** (14), 5316 (2022). <https://doi.org/10.3390/s22145316>
- [60] A. Mukherjee, L.R. Jaidev, K. Chatterjee, A. Misra. *Nano Express*, **1**, 010003 (2020). DOI: 10.1088/2632-959X/ab7491
- [61] Y. Zhou, C. Gao, Y. Guo. *J. Mater. Chem. A*, **6**, 10286 (2018). DOI: 10.1039/C8TA02679C
- [62] Y. Masuda. *Sensors Actuators B: Chem.*, **364**, 131876 (2022). DOI: 10.1016/j.snb.2022.131876
- [63] S.T. Navale, M.A. Chougule, V.B. Patil, A.T. Mane. *Synth. Met.*, **189**, 94 (2014). DOI: 10.1016/j.synthmet.2014.01.002
- [64] M.G. Chung, D.H. Kim, H.M. Lee, T. Kim, J.H. Choi, D.K. Seo, J.-B. Yoo, S.-H. Hong, T.J. Kang, Y.H. Kim. *Sensors Actuators B: Chem.*, **166–167**, 172 (2012). DOI: 10.1016/j.snb.2012.02.036
- [65] V.I. Sysoev, A. Okotrub, I. Asanov, P. Gevko, L. Bulusheva. *Carbon*, **118**, 225 (2017). DOI: 10.1016/j.carbon.2017.03.026
- [66] V.I. Sysoev, M.O. Bulavskiy, D.V. Pinakov, G.N. Chekhova, I.P. Asanov, P.N. Gevko, L.G. Bulusheva, A.V. Okotrub. *Materials*, **13** (16), 3538 (2020). DOI: 10.3390/ma13163538

Translated by M. Verenikina